Supporting Information

Decoding In-Cell Respiratory Enzyme Dynamics by Label-Free *In-situ* Electrochemistry

Yoshihide Tokunou[1,2] * , Tomohiko Yamazaki [2,3], Takashi Fujikawa[2], and Akihiro Okamoto[1,2,4,5,6] *

1. Department of Life and Environmental Sciences, University of Tsukuba, 1-1-1 Tennodai, Tsukuba, Ibaraki 305-8572, Japan.
2. Research Center for Macromolecules and Biomaterials, National Institute for Materials Science, 1-2-1 Sengen, Tsukuba, Ibaraki, 305-0047, Japan
3. School of Life Science, Hokkaido University, 10 Kita, 8 Nishi, Kita-ku, Sapporo, Hokkaido 060-0808, Japan
4. International Center for Materials Nanoarchitectonics, National Institute for Materials Science, 1-1 Namiki, Tsukuba, Ibaraki 305-0044, Japan.
5. School of Chemical Sciences and Engineering, Hokkaido University, 13 Kita, 8 Nishi, Kita-ku, Sapporo, Hokkaido 060-8628, Japan.
6. Institute of Innovation for Future Earth and Laboratory for Integrated Science and Materials, Tokyo Institute of Technology, 4259 Nagatsuta-cho, Midori-ku, Yokohama, Kanagawa 226-8503, Japan

*: corresponding author

Y. T.: tokunou.yoshihide.ga@u.tsukuba.ac.jp

A. O.: okamoto.akihiro@nims.go.jp

Contents:

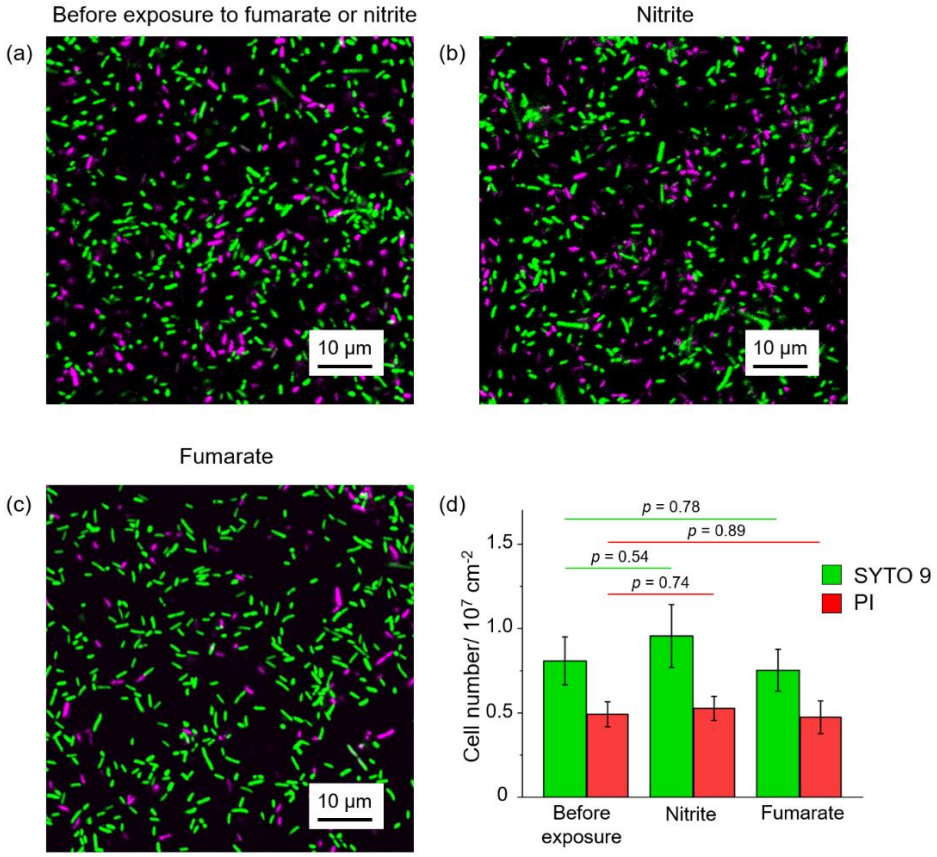

Figure S1. Representative confocal microscopic images of *S. oneidensis* MR-1 cells on ITO electrodes before exposure to nitrite or fumarate (a), after exposure to 5.0 mM nitrite for 1 h (b), and after exposure to 3.0 mM fumarate for 1 h (c), in DM containing 10 μM riboflavin. The images were obtained by confocal fluorescence microscopy (LSM880, Carl Zeiss) equipped with a 63× water-dipping objective lens following SYTO 9 (excitation, 488 nm; emission, 505–545 nm) and propidium iodide (PI) staining (excitation, 543 nm; emission, 620–660 nm). (d) The number of live cells (stained by SYTO 9) and dead cells (stained by PI) on ITO electrodes under conditions of (a)~(c). Error bars represent the mean ± SEM for five individual images obtained from different reactors. P-values from unpaired two-tailed Student's t-tests were used to compare the images before and after exposure to nitrite or fumarate.

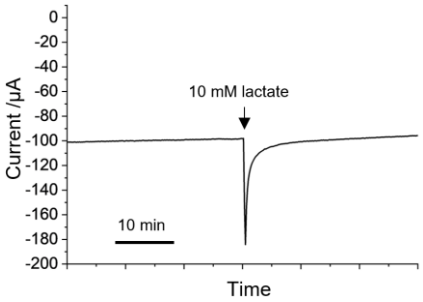

Figure S2. A representative time course for cathodic current under potential application at −0.45 V (vs. SHE) in the presence of electrode-attached *S. oneidensis* MR-1 cells, 10 μM riboflavin, and 5.0 mM fumarate. The arrow indicates the timing of 10 mM lactate addition.

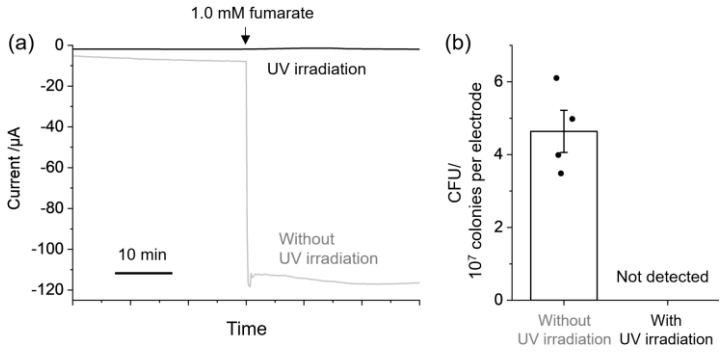

Figure S3. (a) Representative time courses for cathodic current under potential application at −0.45 V (vs. SHE) in the presence of electrode-attached *S. oneidensis* MR-1 cells and 10 μM riboflavin. The black line represents the cathodic current after the irradiation of UV to the electrode for 1 h. The gray line represents the data without UV irradiation, which is the same with the blue line in Figure 1d. (b) Colony formation unit (CFU) of *S. oneidensis* MR-1 cells on each electrode with or without UV irradiation. CFU after UV irradiation was not detectable (below 1000 CFU per electrode).

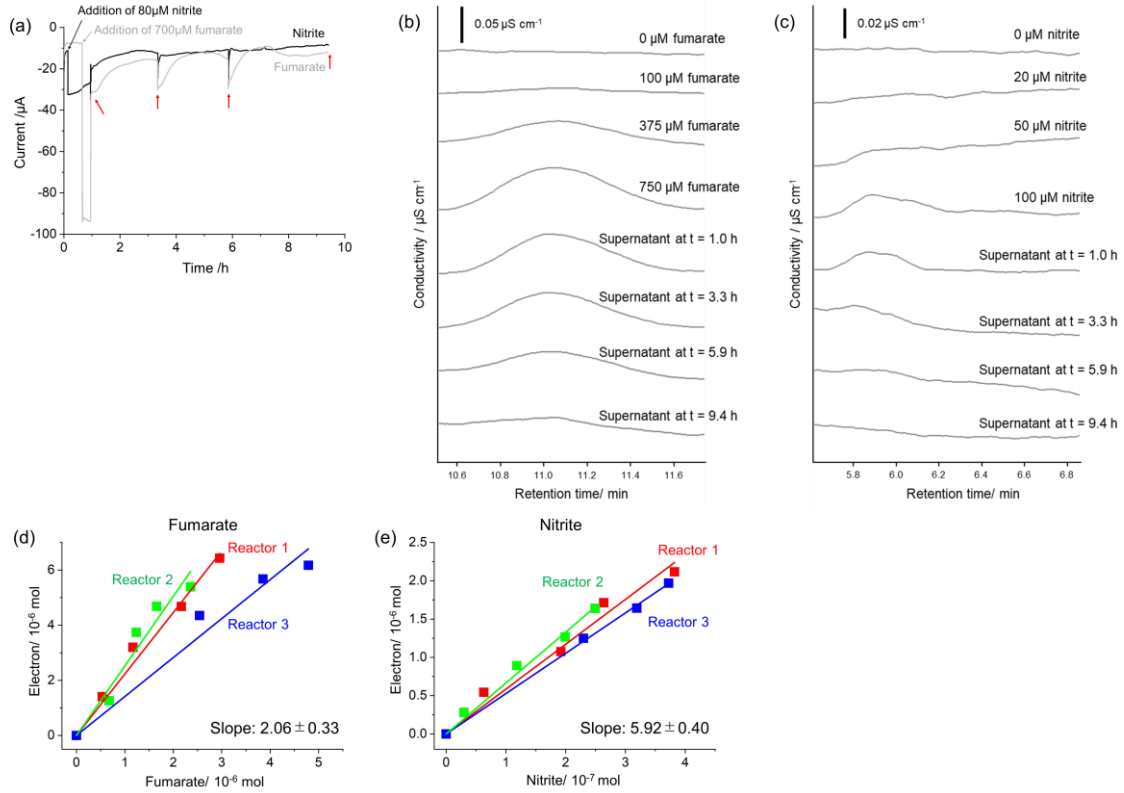

Figure S4. (a) Representative time courses for cathodic current from electrode-attached *S. oneidensis* MR-1 cells under potential application at −0.45 V (vs SHE) with 10 μM riboflavin when supernatant was sampled for ion chromatography to quantify nitrite and fumarate. The black arrow indicates the timing of 80 μM nitrite or 700 μM fumarate addition, and the red arrows indicate the timings of shaking reactors and sampling supernatant. (b, c) Ion chromatograms of supernatant, which were sampled in (a). (b) and (c) represents the chromatograms of fumarate and nitrite, respectively. The concentrations of fumarate and nitrite were calculated from the area of peaks at 11.0 min and 5.9 min, respectively. Plots of the number of electrons delivered to MR-1 cells against (d) fumarate or (e) nitirite consumption at an electrode potential of −0.45 V (vs SHE), which are examined in three independent reactors. The baseline current was subtracted from the electron number. The cathodic current profile in (a) was translated into the "Reactor 1" data. The plots of "Reactor 1" are identical to the plots of Figure 1e. The error bars for slopes represent the mean±SEM obtained from three separate experiments.

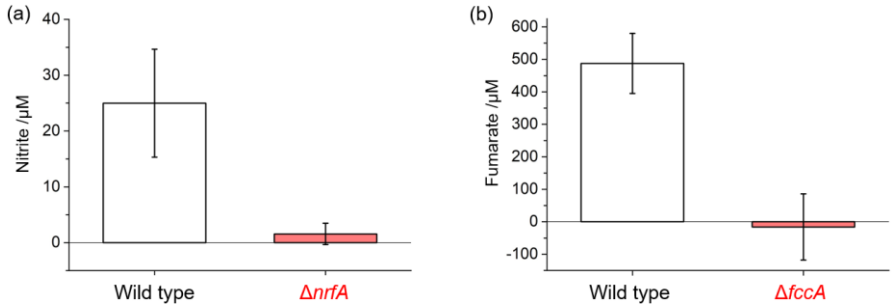

Figure S5. The extent of (a) nitrite consumption and (b) fumarate consumption after potential application at −0.45 V (vs SHE) for 30 min to cells-attached ITO electrodes. The initial concentrations of nitrite and fumarate are 0.1 mM and 1.0 mM, respectively. The concentration of nitrite and fumarate was quantified by ion chromatography. The error bars for slopes represent the mean±SEM obtained from three separate experiments.

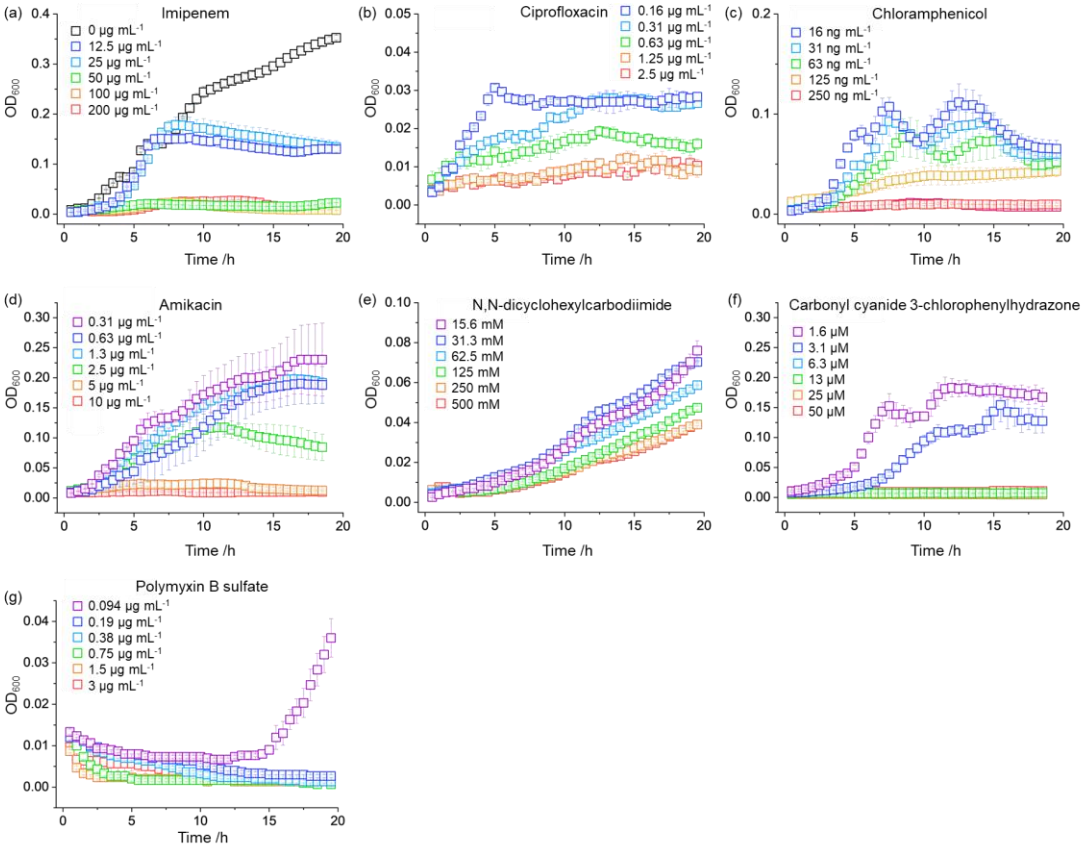

Figure S6. The effect of antibiotics and inhibitors on the growth of *Shewanella oneidensis* MR-1. *S. oneidensis* MR-1 cells at OD_{600} of 0.01 were grown in the defined medium containing 10 mM lactate and each antibiotic/inhibitor aerobically at 303 K, and OD_{600} was recorded at each time point. The error bars represent the mean±SEM obtained from three separate cultures.

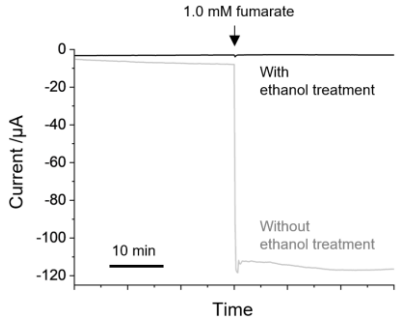

Figure S7. Time courses for cathodic current under potential application at −0.45 V (vs. SHE) in the presence of electrode-attached *S. oneidensis* MR-1 cells and 10 μM riboflavin. The black line represents the cathodic current after the treatment with ethanol for 10 min. The gray line represents the data without ethanol treatment, which is the same with the blue line in Figure 1d.

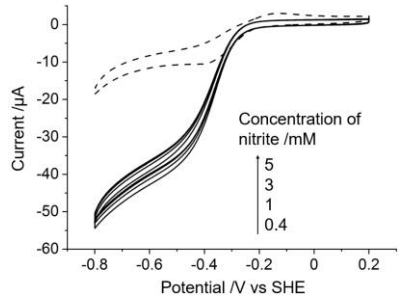

Figure S8. Cyclic voltammograms (CV) of *Shewanella oneidensis* MR-1 cells on an ITO electrode in the presence of 10 μM riboflavin with nitrite (solid lines) and without nitrite (dashed line). The concentration of nitrite is indicated. The scan rate is 10 mVs^{-1}.

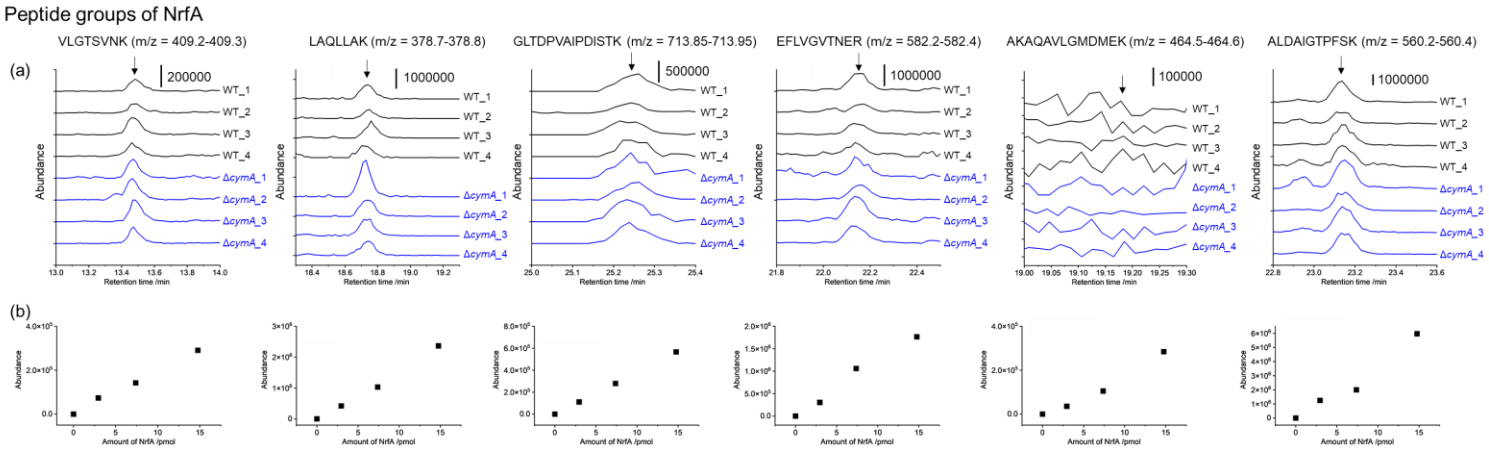

(c)

The amount of NrfA on an ITO electrode estimated from each peptide group abundance /pmol

	VLGTSVNK	LAQLLAK	GLTDPVAIPDISTK	EFLVGVTNER	AKAQAVLGMDMEK	ALDAIGTPFSK	Average
WT_1	4.33	3.72	7.60	5.43	2.43	3.92	4.57
WT_2	3.36	2.08	4.34	2.62	4.50	2.43	3.22
WT_3	6.33	3.77	6.68	3.38	4.65	3.90	4.79
WT_4	4.39	3.20	7.70	3.80	12.4	4.12	5.93
*ΔcymA*_1	6.73	8.76	10.2	5.75	3.08	5.92	6.74
*ΔcymA*_2	7.46	4.52	7.89	4.46	5.43	3.71	5.58
*ΔcymA*_3	7.91	4.54	10.4	7.57	3.17	5.08	6.45
*ΔcymA*_4	5.29	3.73	8.71	5.28	4.32	4.28	5.27

(d)

	The amount of NrfA on an ITO electrode /pmol
WT	4.63 ± 0.55
ΔcymA	6.01 ± 0.35

Figure S9. (a) LC-MS chromatograms of *S. oneidensis* MR-1 cells on ITO electrodes. The chromatograms are specified at the m/z corresponding to each peptide group of NrfA. The arrows indicate the peak of each peptide group identified by Proteome Discoverer. The retention time of each peak was corrected according to ΔApexRT (the error of peak retention time among samples) determined by Proteome Discoverer. (b) Calibration curve of each peptide group using synthesized NrfA. (c) The amount of NrfA on an ITO electrode, estimated from each peptide group abundance in LC-MS chromatograms. (d) The amount of NrfA on an ITO electrode, calculated from four samples.

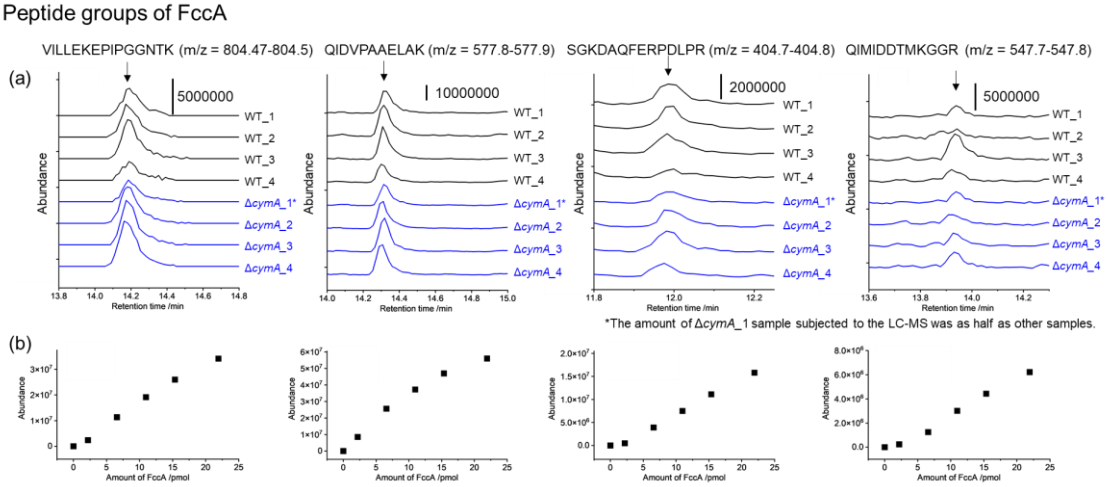

(c)

The amount of FccA on an ITO electrode estimated from each peptide group abundance /pmol

	VILLEKEPIPGGNTK	QIDVPAAELAK	SGKDAQFERPDLPR	QIMIDDTMKGGR	Average
WT_1	3.69	1.84	3.79	5.51	3.71
WT_2	3.79	2.85	3.04	5.04	3.68
WT_3	4.39	2.35	5.60	12.8	6.28
WT_4	1.67	0.11	2.48	7.02	2.82
*ΔcymA*_1	6.08	2.92	5.70	12.7	6.84
*ΔcymA*_2	3.91	1.76	2.83	6.58	3.77
*ΔcymA*_3	4.66	3.11	3.10	7.15	4.50
*ΔcymA*_4	4.76	2.60	3.86	8.28	4.87

(d)

	The amount of FccA on an ITO electrode /pmol
WT	4.12 ± 0.75
ΔcymA	5.00 ± 0.66

Figure S10. (a) LC-MS chromatograms of *S. oneidensis* MR-1 cells on ITO electrodes. The chromatograms are specified at the m/z corresponding to each peptide group of FccA. The arrows indicate the peak of each peptide group identified by Proteome Discoverer. The retention time of each peak was corrected according to ΔApexRT (the error of peak retention time among samples) determined by Proteome Discoverer. (b) Calibration curves of each peptide group using synthesized FccA. (c) The amount of FccA on an ITO electrode, estimated from each peptide group abundance in LC-MS chromatograms. (d) The amount of FccA on an ITO electrode, calculated from four samples.

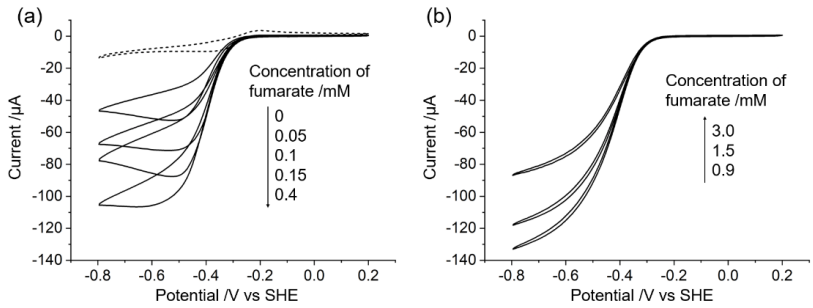

Figure S11. CV of *S. oneidensis* MR-1 cells on an ITO electrode with 0 ~ 0.4 mM fumarate (a) and 0.9 ~ 3.0 mM fumarate (b) in the presence of 10 μM riboflavin and 6.0 mg L^{-1} polymyxin B. Scan rate is 10mVs^{-1}.

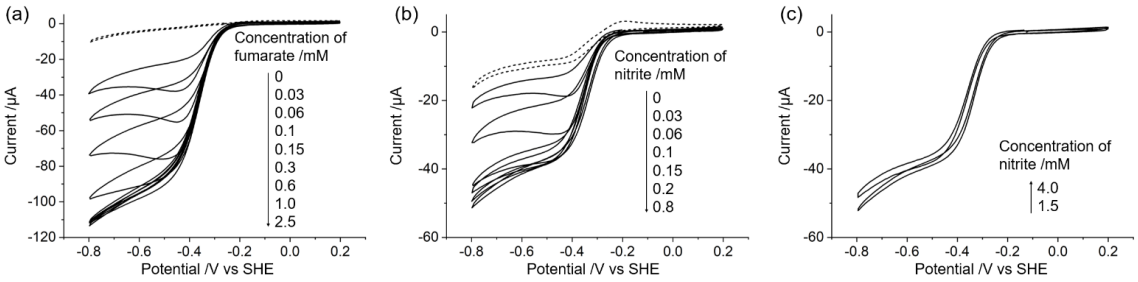

Figure S12. CV of Δ*cymA* cells on an ITO electrode with fumarate (a) and nitrite (b, c) in 10 μM riboflavin. Scan rate is 10 mVs^{-1}.

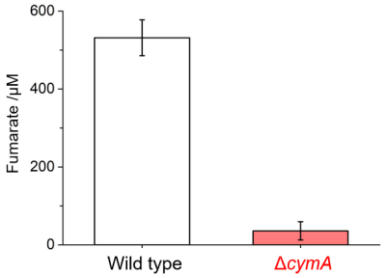

Figure S13. The amount of consumed fumarate by *S. oneidensis* MR-1 cells WT and Δ*cymA* during 90 min cultivation. Cells at OD_{600} of 0.2 were incubated in anaerobic DM containing 10 mM lactate and 500 μM fumarate as the sole electron donor and acceptor, respectively.

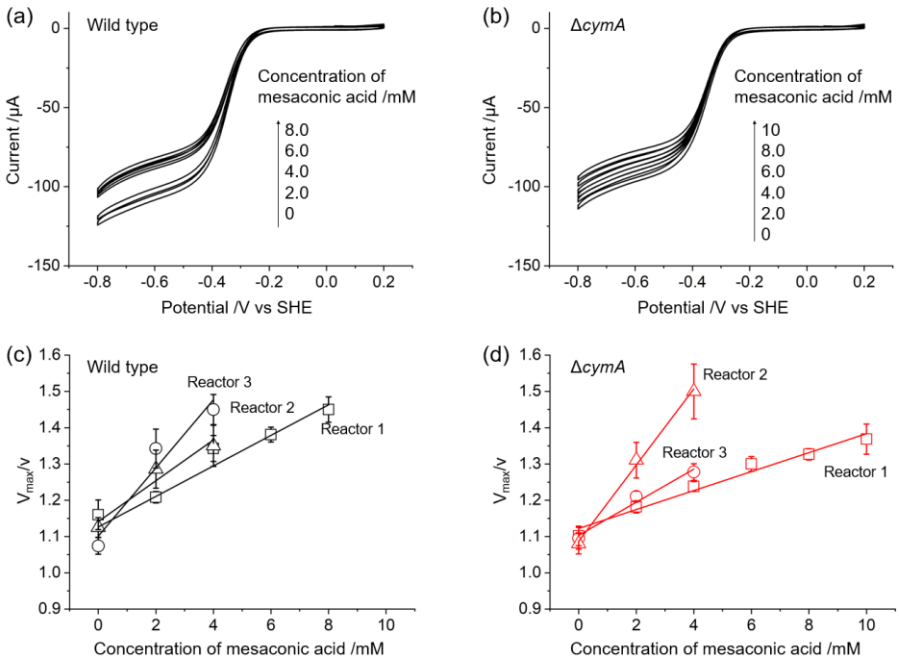

Figure S14. The impact of fumarate reductase inhibitor on the cathodic current of *S. oneidensis* MR-1 cells on an ITO electrode. CV of *S. oneidensis* MR-1 cells wild type (a) and Δ*cymA* (b) in the presence of 5.0 mM fumarate and 10 μM riboflavin with various concentrations of mesaconic acid. Scan rate is 10 mVs^{-1}. Plots of V_{max}/v against the concentration of mesaconic acid for wild type (c) and Δ*cymA* (d). Experiments were conducted three times in separate reactors. v was obtained from the cathodic limiting current after subtraction by that in the absence of fumarate and V_{max} was set as 145 μA. The slopes were 0.0626 ± 0.0166 and 0.0589 ± 0.0237, respectively. The CV data in (a) and (b) were translated into the "Reactor 1" data.

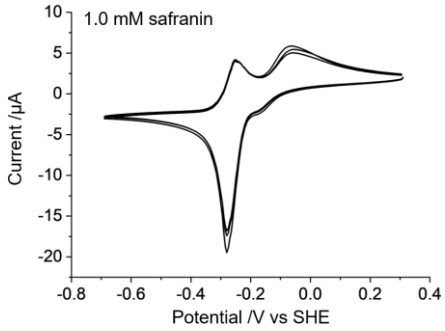

Figure S15. Representative CVs of 1.0 mM safranin, measured in three independent wells of the high-throughput electrochemical system. The redox peak pair with the redox potential at -0.27 V vs. SHE is identical with that reported previously (Y. Choi *et al, Bull. Kor. Chem. Soc.* 24, 437-440 (2003)). The scan rate is 5 mVs^{-1}.

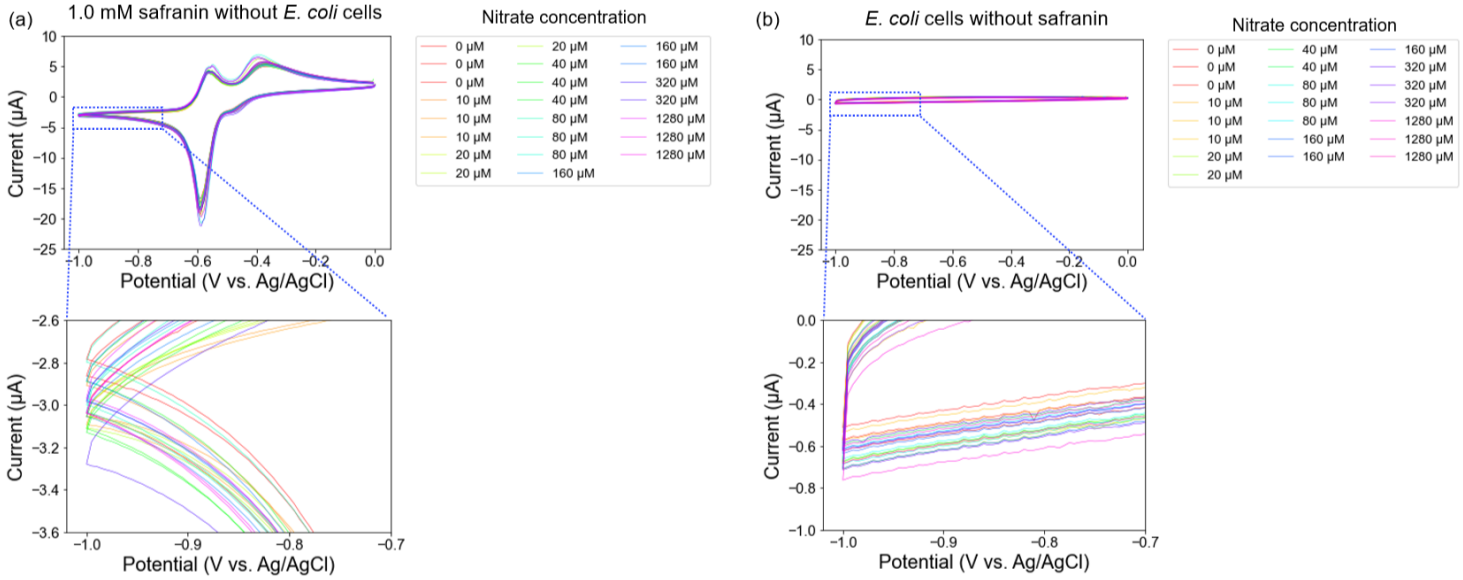

Figure S16. CVs measured in the high-throughput electrochemical system. (a) CVs of 1.0 mM safranin without *E. coli* cells. (b and c) CVs of *E. coli* cells without safranin. The concentrations of nitrate are indicated. The scan rate is 5 mVs^{-1}.

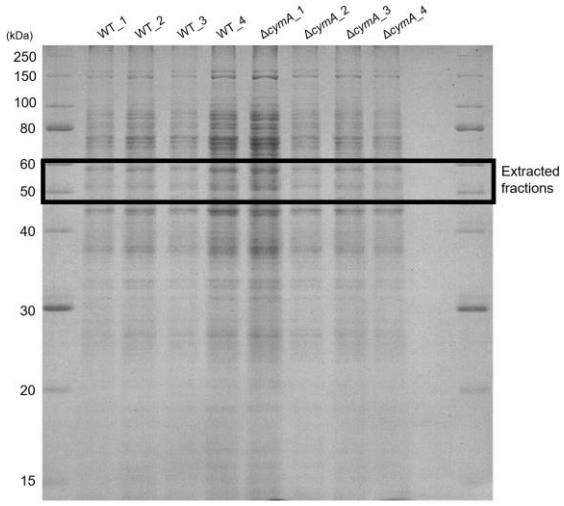

Figure S17. SDS-PAGE of *S. oneidensis* MR-1 cells on ITO electrodes for extraction of NrfA. One-eighth of cell lysate from each ITO electrode was applied to SDS-PAGE. The fractions corresponding to about 45-60 kDa were extracted and utilized as LC-MS samples. The total protein amount on each ITO electrode was estimated to be about ~10^{-4} g scale by BCA assay.

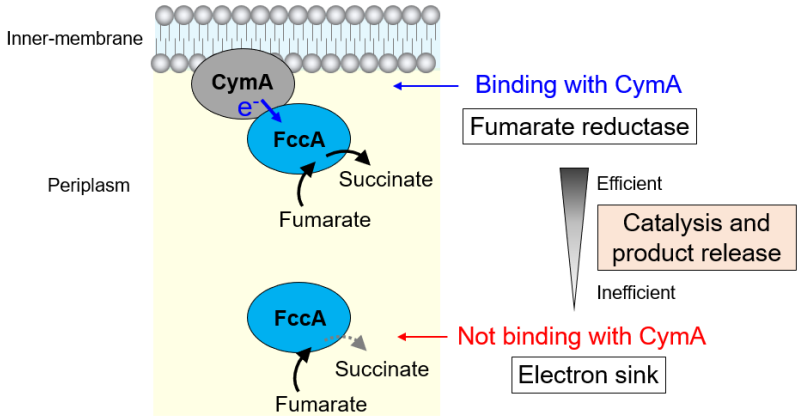

Figure S18. A proposed model of two roles in FccA dictated by association with CymA in MR-1 cells.

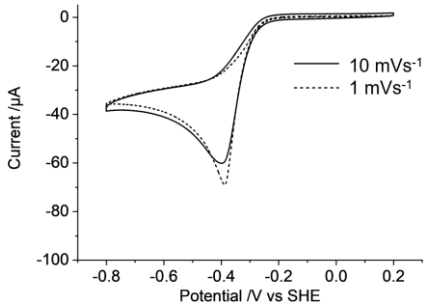

Figure S19. CV of *S. oneidensis* MR-1 cells in the presence of 0.075 mM fumarate with a scan rate of 10 mVs^{-1} (solid line) and 1 mVs^{-1} (dashed line), showing almost identical cathodic current at −0.8 V vs SHE.

Table S1. Peptide groups used for quantification of FccA and NrfA by LC-MS/MS

	Sequence
NrfA	VLGTSVNK
	LAQLLAK
	GLTDPVAIPDISTK
	EFLVGVTNER
	AKAQAVLGMDMEK
	ALDAIGTPFSK
FccA	VILLEKEPIPGGNTK
	QIDVPAAELAK
	SGKDAQFERPDLPR
	QIMIDDTMKGGR